molecular pharmaceutics

ARTICLE

pubs.acs.org/molecularpharmaceutics

Double-Transduced MDCKII Cells To Study Human P-Glycoprotein (ABCB1) and Breast Cancer Resistance Protein (ABCG2) Interplay in Drug Transport across the Blood−Brain Barrier

Birk Poller, Els Wagenaar, Seng Chuan Tang, and Alfred H. Schinkel*

Division of Molecular Biology, The Netherlands Cancer Institute, Amsterdam, The Netherlands

Supporting Information

ABSTRACT: P-glycoprotein (P-gp/ABCB1) and breast cancer resistance protein (BCRP/ABCG2) combination knockout mice display disproportionately increased brain penetration of shared substrates, including topotecan and several tyrosine kinase inhibitors, compared to mice deficient for only one transporter. To better study the interplay of both transporters also *in vitro*, we generated a transduced polarized MDCKII cell line stably coexpressing substantial levels of human ABCB1 and ABCG2 (MDCKII-ABCB1/ABCG2). Next, we measured concentration-dependent transepithelial transport of topotecan, sorafenib and sunitinib. By blocking either one or both of the transporters simultaneously, using specific inhibitors, we aimed to mimic the ABCB1-ABCG2 interplay at the blood−brain barrier in wild-type, single or combination knockout mice. ABCB1 and ABCG2 contributed to similar extents to topotecan transport, which was only partly saturable. For sorafenib transport, ABCG2 was the major determinant at low concentrations. However, saturation of ABCG2-mediated transport occurred at higher sorafenib concentrations, where ABCB1 was still fully active. Furthermore, sunitinib was transported equally by ABCB1 and ABCG2 at low concentrations, but ABCG2-mediated transport became saturated at lower concentrations than ABCB1-mediated transport. The relative impact of these transporters can thus be affected by the applied drug concentrations. A comparison of the *in vitro* observed (inverse) transport ratios and cellular accumulation of the drugs at low concentrations with *in vivo* brain penetration data from corresponding *Abcb1a/1b*$^{-/-}$, *Abcg2*$^{-/-}$ and *Abcb1a/1b;Abcg2*$^{-/-}$ mouse strains revealed very similar qualitative patterns for each of the tested drugs. MDCKII-ABCB1/ABCG2 cells thus present a useful *in vitro* model to study the interplay of ABCB1 and ABCG2.

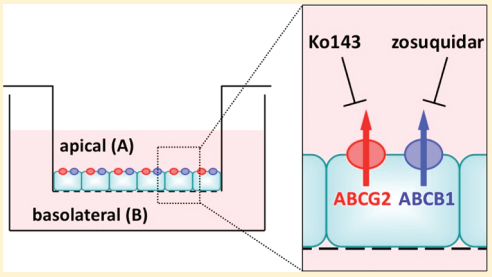

KEYWORDS: MDCKII, ABCB1, ABCG2, tyrosine kinase inhibitor, blood−brain barrier

INTRODUCTION

P-glycoprotein (P-gp/ABCB1) and breast cancer resistance protein (BCRP/ABCG2), both members of the ATP-binding cassette (ABC) transporter family, are expressed at the apical membranes of various polarized cells such as intestinal enterocytes, hepatocytes, renal epithelial cells and the brain capillary endothelial cells (BCECs) forming the blood−brain barrier (BBB). A variety of drugs, including many anticancer drugs, are subject to active efflux by one or both transporters, potentially resulting in limited gastrointestinal absorption, increased renal or hepatic excretion and limited brain penetration.[1] Besides their physiological expression and functions, ABCB1 and ABCG2 are expressed in many tumor types, mediating multidrug resistance against anticancer drugs.[2]

The protective role of ABCB1 at the BBB is well-established and was first demonstrated directly in *Abcb1a*$^{-/-}$ knockout mice, where ABCB1 significantly restricts the brain entry of various drugs.[3,4] More recently, insight was gained into the efflux activity of ABCG2 at the BBB. In *Abcg2*$^{-/-}$ mice and in Abcb1a mutant (i.e., Abcb1a-deficient) or *Abcb1a/1b*$^{-/-}$ mice, when treated with the dual ABCB1 and ABCG2 inhibitor elacridar (GF120918), increased brain concentrations of imatinib, mitoxantrone and prazosin were found as compared to wild-type (WT) mice.[5,6] As a variety of drugs are shared substrates of ABCB1 and ABCG2, the generation of an *Abcb1a/1b;Abcg2*$^{-/-}$ combination knockout mouse model allowed the study of the interplay between both transporters at the BBB. This model was applied to study the pharmacokinetic profiles, in particular brain penetration, of the ABCB1 and ABCG2 cosubstrates topotecan and imatinib.[7,8] Whereas, compared to WT mice, only a modest increase in topotecan and imatinib brain accumulation was observed in the single-transporter knockout mice, brain accumulation was disproportionately increased in *Abcb1a/1b;Abcg2*$^{-/-}$ mice (i.e., several-fold higher than the sum of the increases in *Abcb1a/1b*$^{-/-}$ and *Abcg2*$^{-/-}$ mice). These data suggest that the remaining transporter, which is still present in single-transporter knockout mice, can often largely compensate for the loss of function of the knocked-out transporter. In subsequent studies, similar effects were found for a variety of drugs, including several tyrosine kinase inhibitors (TKI) such as lapatinib, dasatinib, sorafenib, gefitinib, erlotinib[9−14] and very recently sunitinib.[15]

Received: November 15, 2010
Accepted: February 10, 2011
Revised: February 7, 2011
Published: February 10, 2011

While for some of the drugs, including topotecan and imatinib, both transporters appeared to contribute more or less equally to the efflux activity at the BBB, the brain penetration of dasatinib and sunitinib appeared to be mainly limited by ABCB1. In comparison, the brain accumulation of sorafenib was mainly restricted by ABCG2. Collectively, these studies raised the question whether the observed effects in the *Abcb1a/1b;Abcg2*$^{-/-}$ mice are based on an additive or a synergistic interaction between ABCB1 and ABCG2 at the BBB.

All data generated so far on the interaction between ABCB1 and ABCG2 were based on *in vivo* studies. The lack of an *in vitro* system with simultaneously high expression levels of ABCB1 as well as ABCG2 impeded mechanistic studies of this interaction at the cellular level. Therefore, we aimed to generate a double-transduced Madin-Darby canine kidney (MDCKII) cell line stably overexpressing human ABCB1 and ABCG2 and use it to study the transepithelial transport of shared substrates, in this study represented by topotecan, sorafenib and sunitinib. By blocking either one or both transport proteins with specific inhibitors in MDCKII-ABCB1/ABCG2 cells, we aimed to mimic the ABCB1-ABCG2 interaction at the BBB in WT, *Abcb1a/1b*$^{-/-}$, *Abcg2*$^{-/-}$ and *Abcb1a/1b;Abcg2*$^{-/-}$ mice, respectively. Moreover, we performed transport experiments in a concentration-dependent manner to study possible saturation effects of the efflux proteins. We further compared the *in vitro* transport data of our test compounds with previously generated *in vivo* brain penetration results.

MATERIALS AND METHODS

Chemicals and Cell Lines. [^{3}H]Sorafenib (0.17 Ci/mmol) was from Moravek Biochemicals (Brea, CA), [^{3}H]sunitinib (12.5 Ci/mmol) was from American Radiolabeled Chemicals (St. Louis, MO) and [^{14}C]inulin (5.6 Ci/mol) was from Amersham Biosciences (Little Chalfont, U.K.). [^{14}C]Topotecan (13.0 Ci/mol) (Smith-Kline Beecham Pharmaceuticals (King of Prussia, PA) and zosuquidar (LY-335979) (Eli Lilly, Indianapolis, IN, USA) were a kind gift of Dr. O. van Tellingen (The Netherlands Cancer Institute, Amsterdam, NL). Sorafenib, sunitinib and topotecan were purchased from Sequoia Research Products (Pangborne, U.K.). Ko143 was described previously.[16] All other chemicals were of analytical grade and obtained from standard suppliers unless mentioned otherwise. Rat monoclonal antibody BXP-53 recognizing ABCG2/Abcg2 and mouse monoclonal antibody C219 recognizing ABCB1 were from Abcam (Cambridge, MA). Adherent embryo fibroblast cells MEF3.8 overexpressing human ABCG2 were described and characterized previously.[17] The polarized MDCKII parental cell line and a subclone transduced with human ABCB1 were described elsewhere.[18] All MDCKII cell lines were cultured in Dulbecco's modified Eagle's medium with high-glucose and GlutaMax (Invitrogen, Carlsbad, CA) supplemented with 10% fetal bovine serum, 50 U/mL penicillin and 50 μg/mL streptomycin.

Generation of ABCG2 Single- and ABCB1/ABCG2 Double-Transduced MDCKII Cell Lines. A MDCKII-ABCB1/ABCG2 double-transduced cell line was generated by transducing MDCKII cells stably overexpressing human ABCB1 with human ABCG2 according to Pavek et al.[17] In parallel, parental MDCKII cells were transduced with human ABCG2 in order to obtain a new MDCKII-ABCG2 cell line. In brief, the LZRS-IRES-GFP expression vector containing full-length WT human ABCG2 cDNA was transfected into the amphotropic Phoenix producer cell line by using the calcium phosphate precipitation method. Viral supernatants from these transfected cells were used to transduce MDCKII-ABCB1 or MDCKII parental cells by coincubation in the presence of 5 μg/mL Polybrene. Enhanced green fluorescent protein (eGFP) expression in transduced cells was analyzed by FACS followed by single-cell sorting for GFP positive cells into 96-well plates containing MDCKII-conditioned medium. Subsequently, ABCG2 mRNA and protein expression as well as topotecan transport activity was measured in outgrowing clones and an optimal clone of MDCKII-ABCB1/ABCG2 cells and MDCKII-ABCG2 cells, respectively, was selected for this study. Stable ABCG2 RNA and protein expression as well as topotecan transport activity was regularly verified in both selected clones over a period of 19 culture passages (~10 weeks).

Western Blot. Cells were trypsinized, washed with ice-cold PBS and resuspended in TD buffer (10 mM Tris-HCl, pH 8.0, 0.1% Triton X-100, 10 mM magnesium sulfate, 2 mM $CaCl_2$, 40 U/mL DNase, 1 mM dithiothreitol and protease inhibitor cocktail from Roche, Basel, Switzerland). Cell suspensions were subjected to 3 freeze−thaw cycles and then incubated at 37 °C for 10 min. After centrifugation (14000 rpm for 5 min) the protein concentration in the supernatant was determined using a BCA Protein Assay Kit (Pierce Chemical, Rockford, IL). Then 10 μg of protein was separated on a polyacrylamide gel (6% for ABCB1 and 8% for ABCG2) followed by transfer to a nitrocellulose membrane using the iBlot Dry Blotting Transfer Stack Mini (Invitrogen, Carlsbad, CA) according to the manufacturer's instructions. Equal protein loading was confirmed by Ponceau S staining of the membranes after protein transfer. After blocking for 1 h at room temperature in blocking buffer (PBS with 1% (w/v) bovine serum albumin, 1% (w/v) milk powder and 0.05% (v/v) Tween 20) the membranes were incubated overnight at 4 °C either with the rat monoclonal antibody BXP-53 recognizing ABCG2 or with the mouse monoclonal antibody C219 recognizing ABCB1 (both in a 1:50 dilution in blocking buffer).

Secondary rabbit anti-rat or rabbit anti-mouse antibodies conjugated to horseradish peroxidase (Dako, Copenhagen, Denmark) were used at 1:1000 dilutions in blocking buffer for 1 h at room temperature. The bands were visualized using an ECL detection kit (GE Healthcare, Little Chalfont, Buckinghamshire, U.K.).

Transport Assays. Transport assays were performed using microporous polycarbonate membrane filters (3.0 μm pore size, 24 mm diameter, Transwell 3414, Costar, Cambridge, MA) as previously described with minor modifications.[17] MDCKII parental cells and subclones were seeded at a density of 1.0×10^6 cells per well and were grown for 72 h, including daily medium changes. Two hours before starting the experiment, cells were washed with prewarmed PBS and preincubated with 2 mL of Opti-MEM (Invitrogen, Carlsbad, CA) either alone or containing the ABCB1 inhibitor zosuquidar (5 μM), the ABCG2 inhibitor Ko143 (1 μM) or a combination of both inhibitors at the indicated concentrations. The experiment was started at $t = 0$ by replacing the medium in the donor compartment (either apical or basolateral) with fresh Opti-MEM containing the substrate or the mixture of substrate and inhibitors. [^{14}C]topotecan (0.02 μCi/mL) was used at concentrations of 1.6 μM and 500 μM, where the lower end of the concentration range was limited by the specific radioactivity of the available radioactive topotecan and 500 μM was the highest soluble concentration. As sorafenib

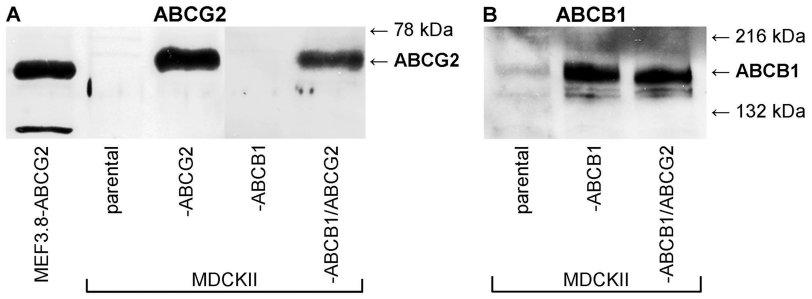

Figure 1. Protein levels of human ABCG2 in MEF3.8-ABCG2 and MDCKII parental, -ABCG2, -ABCB1 and -ABCB1/ABCG2 cells (A). Protein levels of human ABCB1 in MDCKII parental, -ABCB1 and -ABCB1/ABCG2 cells (B). Western blot analysis was performed with 10 μg of cellular protein using the monoclonal antibodies BXP-53 recognizing ABCG2 (70 kDa) and C219 recognizing ABCB1 (170 kDa). Equal protein loading was confirmed by Ponceau S staining of the membranes after protein transfer (data not shown).

showed high nonspecific binding to plastic material in Opti-MEM, all sorafenib experiments were performed in DMEM supplemented with 10% FBS instead of Opti-MEM. [^{3}H]Sorafenib (0.045 μCi/mL) was used in concentrations of 0.3, 2, 10, and 20 μM, [^{3}H]sunitinib (0.045 μCi/mL) in concentrations of 0.02, 0.2, 2, and 20 μM. For [^{3}H]sorafenib and [^{3}H]sunitinib experiments [^{14}C]inulin (0.045 μCi/mL) was added to the experimental solution to check the integrity of the cell monolayer. For [^{14}C]topotecan experiments [^{14}C]inulin leakage was measured in parallel in cells seeded and cultured under the same conditions. Inulin leakage was accepted up to 1% per hour. Aliquots of 50 μL were taken every hour from the acceptor compartment up to 4 h, and radioactivity was measured by liquid scintillation counting. At the end of the experiment filters with cell layers were washed twice with ice-cold PBS and excised and radioactivity was measured. The percentage of substrate appearing in the acceptor compartment relative to the total amount added to the donor compartment at the beginning of the experiment was calculated and plotted in the figures. Transport ratios (r) were calculated by dividing apically directed translocation (BA) by basolaterally directed translocation (AB) of drugs. The relative cellular drug uptake was determined by dividing the amount of radioactivity measured in cell and filters by the initially applied amount of radioactivity. All data points are means (n = 3) ± standard deviation (SD), and two-sided unpaired Student's t test was used to compare AB- and BA-translocation at 4 h.

RESULTS

Generation and Characterization of ABCG2 Single- and ABCB1/ABCG2 Double-Transduced MDCKII Cell Lines. The MDCKII cell line overexpressing human ABCG2 is a commonly used tool to study ABCG2-mediated drug transport.[17,19,20] We generated an ABCB1/ABCG2 double-transduced MDCKII cell line, by transducing MDCKII cells overexpressing ABCB1[21] with human ABCG2. Moreover, because we recently encountered unstable expression and activity of the ABCG2 protein in our original MDCKII-ABCG2 clone, we also generated new ABCG2-overexpressing MDCKII clones. Optimal clones were selected by testing protein levels and transport activity over a number of culture passages.

Western blot analysis revealed substantial protein expression of human ABCG2 in the selected ABCG2 and ABCB1/ABCG2 clones, whereas no expression was observed in MDCKII parental and ABCB1 cells (Figure 1A). Slightly higher ABCG2 protein expression was found in the single-overexpressing ABCG2 clone than in the double-transduced ABCB1/ABCG2 clone. Stably transduced MEF3.8-ABCG2 cells (immortalized fibroblasts which overexpress functionally active human ABCG2) were used as a positive control.[17] Size differences of the main bands between MEF3.8 and MDCKII clones likely represent differences in level of N-glycosylation between the different cell types. Immunoblotting revealed bands of comparable intensities for ABCB1 protein in MDCKII-ABCB1 cells and in the double-transduced ABCB1/ABCG2 clone, indicating that the transduction process had not altered ABCB1 protein expression (Figure 1B).

Functional activity of MDCKII-ABCG2 and -ABCB1/ABCG2 cell lines was assessed by measuring transepithelial transport of topotecan, a cosubstrate of ABCB1 and ABCG2 (results described in the next section). Using zosuquidar in all topotecan transport experiments in order to inhibit endogenous canine ABCB1 in MDCKII-ABCG2 cells as well human ABCB1 in MDCKII-ABCB1/ABCG2 cells allowed us to study the ABCG2-mediated transport in both cell lines. Over a period of 19 culture passages (~10 weeks) we consistently observed clear ABCG2 protein expression as well as substantial ABCG2-mediated topotecan transport activity in both cell lines. During this period no significant alterations of either protein expression or transport activity were observed, indicating stable ABCG2 activity in these lines.

Topotecan Transport in MDCKII Parental, -ABCB1 and -ABCG2 Cells. We first determined transepithelial transport of the shared ABCB1 and ABCG2 substrate [^{14}C]topotecan through monolayers of the MDCKII-ABCB1 and -ABCG2 clones (Figure 2). In the parental cells a transport ratio (r) of 2.9 was observed, presumably resulting from transport by endogenous canine ABCB1 (Figure 2A) as previously reported: addition of the specific ABCB1 inhibitor PSC833 (5 μM) completely blocked topotecan transport in parental cells.[17] In ABCB1-overexpressing cells a topotecan transport ratio of 5.7 was observed due to increased apically and decreased basolaterally directed topotecan translocation as compared to the parental cell line (Figure 2B). This transport was abolished by the specific ABCB1 inhibitor zosuquidar (5 μM) (Figure 2D). For cells overexpressing ABCG2 we measured a topotecan transport ratio of 6.9. This ratio was markedly decreased to a value of 1.8 by the specific ABCG2 inhibitor Ko143 (1 μM), revealing the residual endogenous ABCB1 transport activity (Figure 2C,E). Together, these data show that human ABCG2 is functionally active in the new clone, and that its properties are very similar to those of the original ABCG2 cell line,[17] but with better long-term stability of ABCG2 expression. Furthermore, these results demonstrate that zosuquidar and Ko143 can be used as potent and specific inhibitors of

dx.doi.org/10.1021/mp1003898 |*Mol. Pharmaceutics* 2011, 8, 571–582

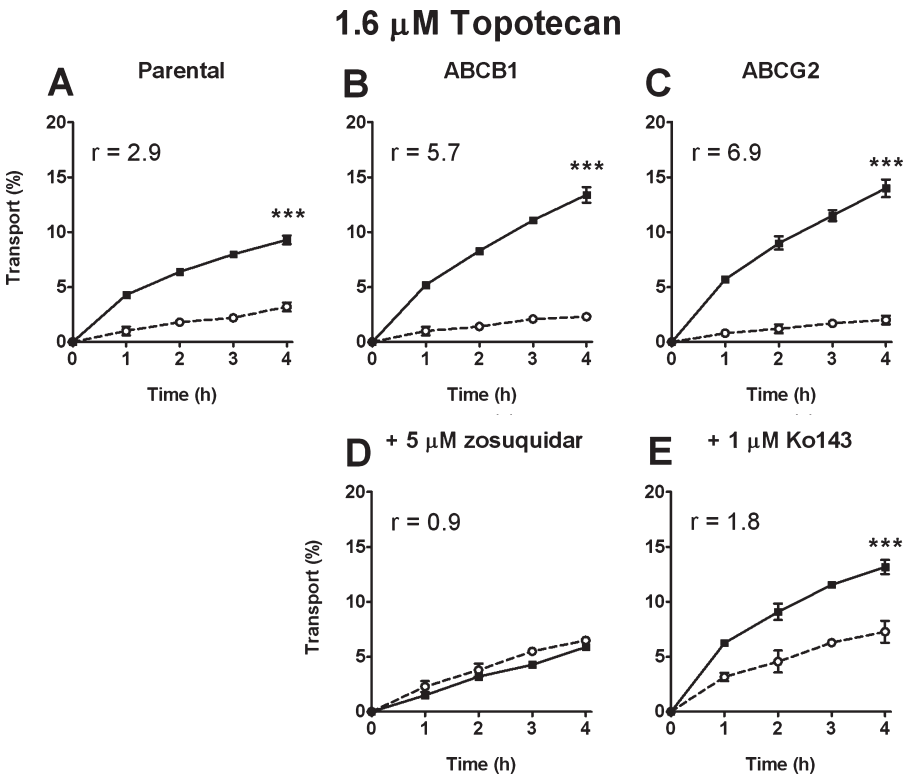

Figure 2. Transepithelial transport of [^{14}C]topotecan at an initial concentration of 1.6 μM through monolayers of MDCKII parental (A), human ABCB1- (B, D), and human ABCG2-transduced cells (C, E). Transport was measured in the absence of inhibitor (A−C) or in the presence of 5 μM zosuquidar to inhibit ABCB1 (D) or 1 μM Ko143 to inhibit ABCG2 (E). Translocation from the apical to the basolateral compartment (open circles), translocation from the basolateral to the apical compartment (filled squares). Results are expressed as mean values ($n = 3$) of relative transport (%) ± SD (error bars are frequently within the symbols). The transport ratio (r) was calculated as the quotient of apically directed and basolaterally directed translocation at 4 h, and differences at 4 h were tested by Student's t test (***: $p < 0.001$).

ABCB1- or ABCG2-mediated topotecan transport, when applied at the used concentrations.

Topotecan Transport in MDCKII-ABCB1/ABCG2 Cells. We subsequently measured topotecan transport in the newly generated double-transduced MDCKII-ABCB1/ABCG2 cell line at topotecan concentrations of 1.6 μM and 500 μM (i.e., close to the limit of solubility in Opti-MEM). The experiments were performed either without inhibitor, in the presence of Ko143 to block ABCG2, in the presence of zosuquidar to inhibit ABCB1, or in the presence of both inhibitors simultaneously (Figure 3). At 1.6 μM topotecan we found a transport ratio of 7.9 under inhibitor-free conditions (Figure 3A). To determine the contribution of ABCB1 to topotecan transport, we applied Ko143, resulting in a transport ratio of 5.3 (Figure 3B). Comparing this ratio with the one observed in the ABCB1 cell line (Figure 2B) demonstrates that transducing these cells with ABCG2 did not alter the activity of ABCB1. Blocking of ABCB1 by zosuquidar revealed the contribution of ABCG2 to topotecan translocation (Figure 3C). The observed ratio of 5.2 indicates significant ABCG2 activity in the double-transduced cell line, and similar to that of ABCB1 in this line. Simultaneous application of both inhibitors abolished active topotecan transport (Figure 3D). When we increased the topotecan concentration to 500 μM we found significantly reduced transport ratios of 5.3 under inhibitor-free conditions and 3.7 in the presence of either Ko143 or zosuquidar, most likely due to beginning saturation of the transporters (Figure 3E,F,G). Topotecan transport at 500 μM was also completely blocked in the presence of both inhibitors (Figure 3H). Taken together, these results indicate that ABCB1- as well as ABCG2-mediated topotecan translocation in the MDCKII-ABCB1/ABCG2 cell line is partially saturable at very high topotecan concentrations. Furthermore, both transporters appear to have high transport capacities for topotecan and to contribute about equally to the active transport over a large concentration range.

Sorafenib Transport in MDCKII-ABCB1/ABCG2 Cells. We next assessed the contribution of ABCB1 and ABCG2 to the transepithelial transport of [^{3}H]sorafenib in a concentration-dependent manner using the MDCKII-ABCB1/ABCG2 cell line. Under uninhibited conditions at 0.3 μM sorafenib we measured a transport ratio of 6.0 representing efficient active sorafenib transport (Figure 4A). Upon specific blocking of ABCG2 using Ko143 we observed a low ABCB1-mediated transport ratio of 1.4 (Figure 4B). Blocking of only ABCB1 by zosuquidar resulted in a transport ratio of 3.7 (Figure 4C) indicating a higher impact of ABCG2 on sorafenib transport compared to ABCB1 at 0.3 μM. Simultaneous addition of Ko143 and zosuquidar completely blocked ABCB1 and ABCG2 activity and even resulted in a slightly higher basolaterally than apically directed translocation (Figure 4D) perhaps due to an apically located uptake system and/or a basolaterally directed efflux transporter of sorafenib.

Upon increasing sorafenib concentrations to 2, 10, and 20 μM without inhibitors, we found reduced transport ratios to 2.8, 1.7 and 1.4, respectively, indicating gradual saturation of active transport (Figure 4A, E, I, M). In the presence of Ko143, ABCB1-mediated sorafenib transport appeared to be at constant

dx.doi.org/10.1021/mp1003898 |*Mol. Pharmaceutics* 2011, 8, 571–582

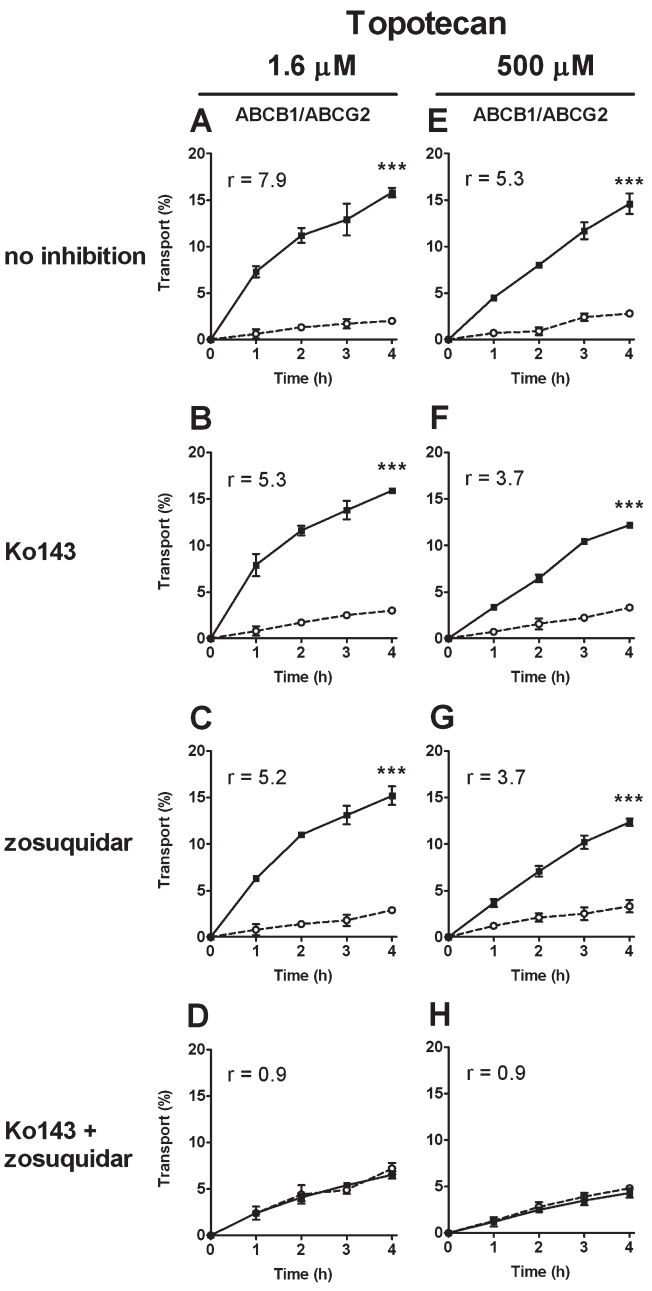

Figure 3. Concentration-dependent transepithelial transport of [^{14}C]topotecan through monolayers of MDCKII-ABCB1/ABCG2 cells. Transport was measured in the absence of inhibitor (A, E), in the presence of 1 μM Ko143 to inhibit ABCG2 (B, F), in the presence of 5 μM zosuquidar to block ABCB1 (C, G) or in the presence of both inhibitors (D, H). [^{14}C]Topotecan was applied at initial concentrations of 1.6 μM (A−D) and 500 μM (E−H) to either apical or basolateral compartments. Translocation from the apical to the basolateral compartment (open circles), translocation from the basolateral to the apical compartment (filled squares). Results are expressed as mean values (n = 3) of relative transport (%) ± SD (error bars are frequently within the symbols). The transport ratio (r) was calculated as described with Figure 2. Differences at 4 h were tested by Student's t test (***: p < 0.001).

levels up to a concentration of 10 μM, while saturation was observed at 20 μM sorafenib (Figure 4B, F, J, N). In contrast, we observed partial saturation of ABCG2-mediated sorafenib transport in the presence of zosuquidar already at a sorafenib concentration of 2 μM, resulting in a reduced transport ratio of 2.0 (Figure 4G). Virtually complete saturation of ABCG2 was found at sorafenib concentrations of 10 μM or higher (Figure 4K, O). These data show a major contribution of ABCG2 to sorafenib transport at 0.3 μM, while the contribution of ABCB1 is rather low. At 2 μM both transporters show similar efficiencies, whereas at 10 μM ABCB1 becomes the more important transporter for sorafenib. Thus, ABCG2 appears to have a higher affinity for sorafenib transport than ABCB1, but this also results in earlier saturation of ABCG2.

Sunitinib Transport in MDCKII-ABCB1/ABCG2 Cells. To examine the contribution of ABCB1 and ABCG2 to sunitinib transport we measured the translocation of [^{3}H]sunitinib in the absence or presence of Ko143 and zosuquidar in the MDCKII-ABCB1/ABCG2 line. The experiments were carried out at sunitinib concentrations of 0.02 (not shown), 0.2, 2, and 20 μM. When no inhibitor was applied we measured significant active transport at a concentration of 0.2 μM resulting in a transport ratio of 4.7 (Figure 5A). Upon blocking ABCG2 with Ko143 we observed an ABCB1-mediated transport ratio of 2.1 (Figure 5B). A similar transport ratio of 2.0 was found for ABCG2-mediated sunitinib transport in the presence of zosuquidar (Figure 5C). Under coincubation with Ko143 and zosuquidar active transport was completely abolished (Figure 5D). Virtually identical transport ratios were observed at a sunitinib concentration of 0.02 μM for all four conditions (data not shown). We therefore conclude that at 0.2 μM we observed completely unsaturated ABCB1- and ABCG2-mediated sunitinib transport. Increasing the sunitinib concentrations to 2 and 20 μM in the absence of inhibitors resulted in lower transport ratios of 3.2 and 2.2, respectively, indicating beginning saturation of the active transport (Figure 5E,I). By studying ABCB1-mediated transport in the presence of Ko143, we found that ABCB1 was only saturable to a small extent with corresponding transport ratios of 2.1, 1.8, and 1.7 at 0.2, 2, and 20 μM, respectively (Figure 5B,F,J). In contrast, beginning saturation of ABCG2-mediated sunitinib transport in presence of zosuquidar was already observed at a concentration of 2 μM. The transport ratio of 2.0 at 0.2 μM was reduced to 1.3 at concentrations of 2 and 20 μM (Figure 5C,G,K). A ratio of about 1 under coincubation with both inhibitors was found at all tested concentrations (Figure 5D,H,L). Thus for sunitinib up to 0.2 μM we observed similar transport contributions of ABCB1 and ABCG2, but at higher sunitinib concentrations (2−20 μM) ABCG2 was more easily saturated than ABCB1. Note that at a concentration of 20 μM sunitinib the apically as well as the basolaterally directed sunitinib translocation was reduced by about 2-fold as compared to concentrations of 2 μM, potentially due to saturated sunitinib uptake in the MDCKII cells. A similar overall reduction of sunitinib translocation was previously seen in LLC-PK cells at 10 μM sunitinib.[22]

Intracellular Accumulation of Sorafenib and Sunitinib in MDCKII-ABCB1/ABCG2 Cells. Besides transepithelial translocation we also measured intracellular accumulation of sorafenib and sunitinib in MDCKII-ABCB1/ABCG2 cells (Figure 6). Intracellular topotecan levels were also tested, but found to be too low under all circumstances (<1%) to draw significant conclusions. Accumulation results obtained after apical application of drugs are presented, and results upon basolateral application were comparable (not shown). We found highly pronounced changes in relative intracellular accumulation of sorafenib and sunitinib, depending on the degree of saturation or

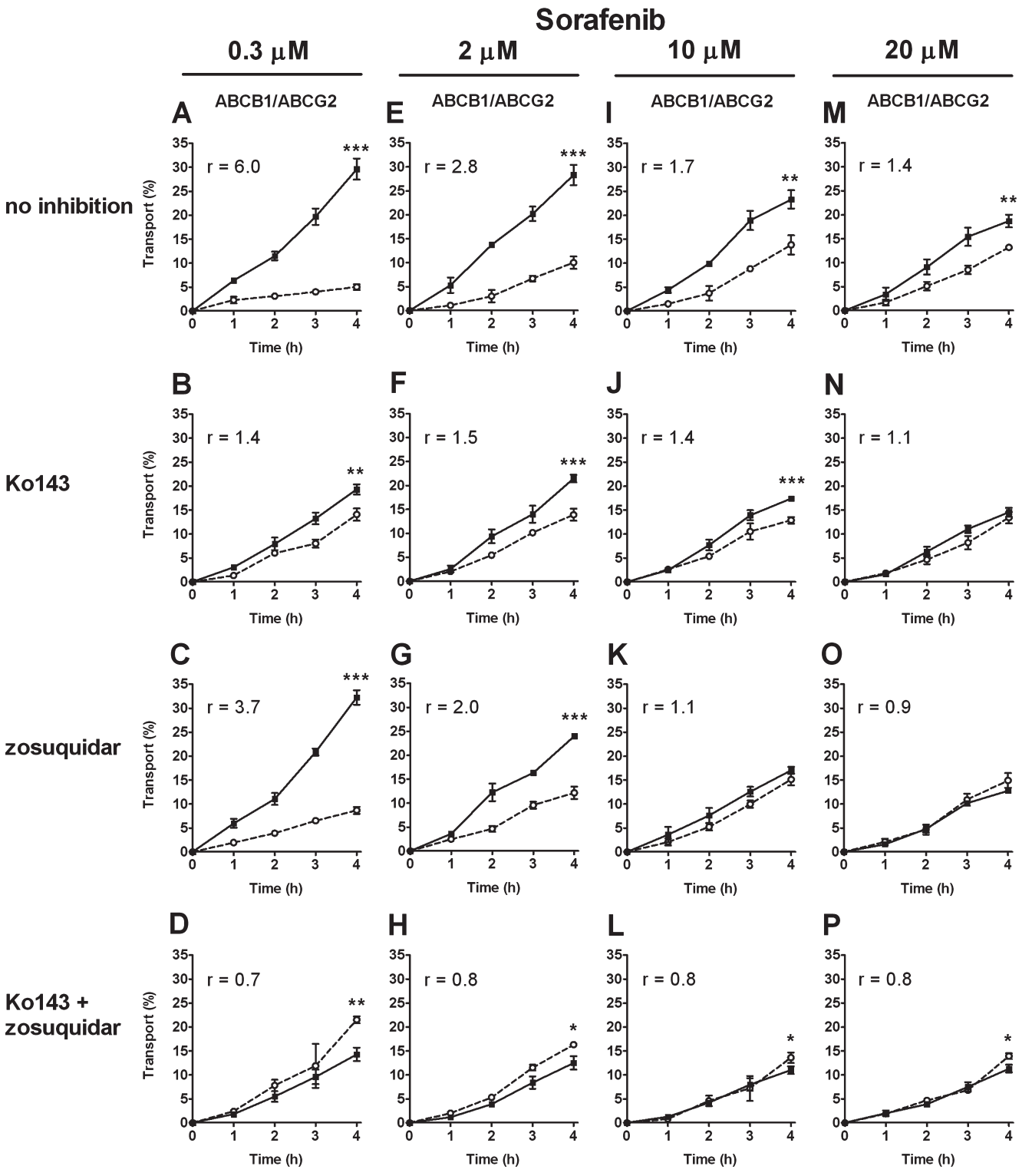

Figure 4. Concentration-dependent transepithelial transport of [^{3}H]sorafenib through monolayers of MDCKII-ABCB1/ABCG2 cells. Transport was measured in the absence of inhibitor (A, E, I, M), in the presence of 1 μM Ko143 to inhibit ABCG2 (B, F, J, N), in the presence of 5 μM zosuquidar to block ABCB1 (C, G, K, O) or in the presence of both inhibitors (D, H, L, P). [^{3}H]Sorafenib was applied at initial concentrations of 0.3 μM (A−D), 2.0 μM (E−H), 10 μM (I−L) and 20 μM (M−P) to either apical or basolateral compartments. Note that no significant polarized sorafenib transport was observed in parental MDCKII cells, indicating a negligible transport contribution of endogenous canine ABCB1.[11] Translocation from the apical to the basolateral compartment (open circles), translocation from the basolateral to the apical compartment (filled squares). Results are expressed as mean values ($n = 3$) of relative transport (%) ± SD (error bars are frequently within the symbols). The transport ratio (r) was calculated as described with Figure 2. Differences at 4 h were tested by Student's t test (*: $p < 0.05$, **: $p < 0.01$, ***: $p < 0.001$).

inhibition of ABCB1 and/or ABCG2. While both transporters were active at a sorafenib concentration of 0.3 μM, only 3.2% of the initially applied drug was found within the cells (Figure 6A). This value was increased by 4.6- or 1.6-fold in the presence of

dx.doi.org/10.1021/mp1003898 |Mol. Pharmaceutics 2011, 8, 571–582

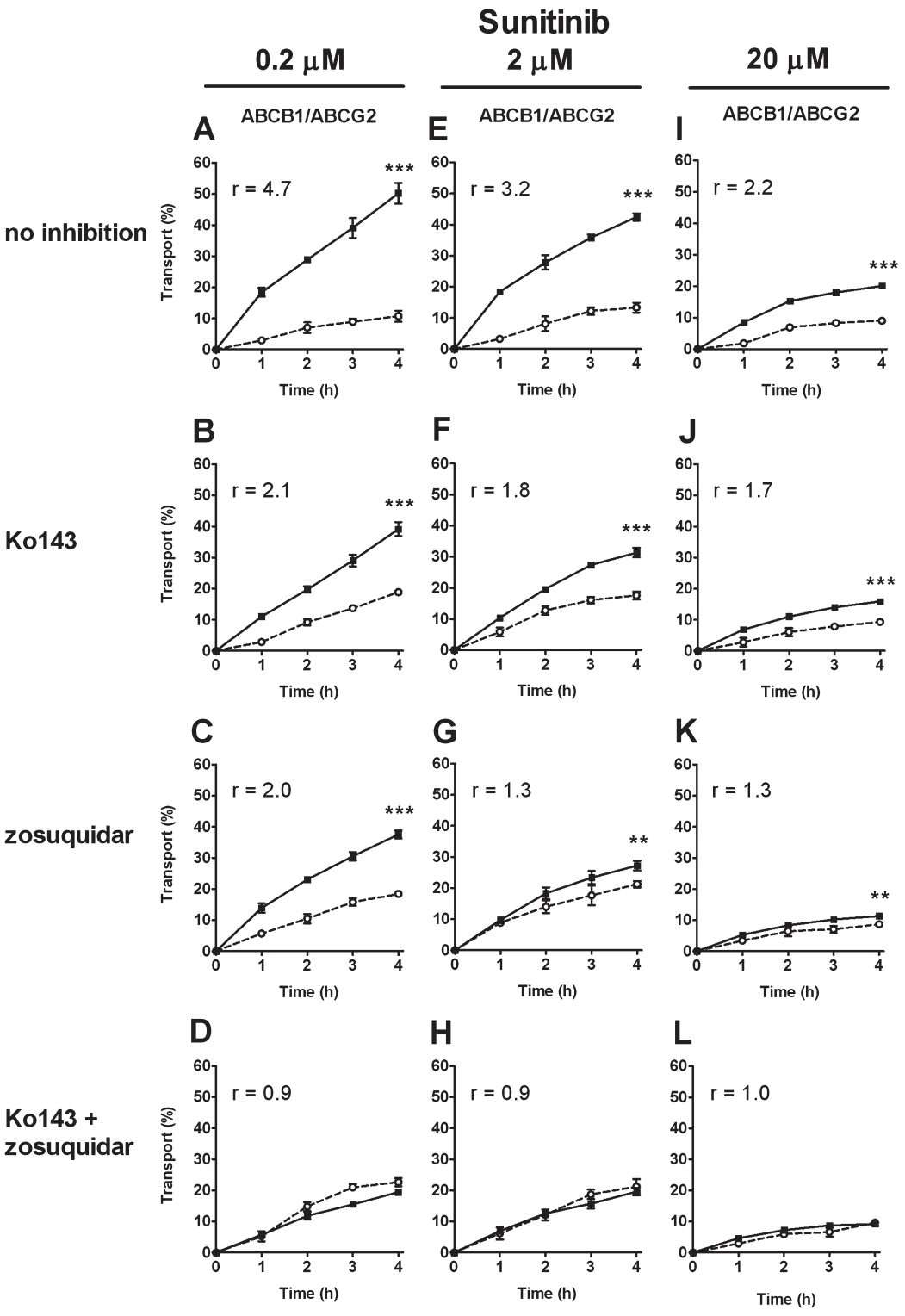

Figure 5. Concentration-dependent transepithelial transport of [^{3}H]sunitinib through monolayers of MDCKII-ABCB1/ABCG2 cells. Transport was measured in the absence of inhibitor (A, E, I), in the presence of 1 μM Ko143 to inhibit ABCG2 (B, F, J), in the presence of 5 μM zosuquidar to block ABCB1 (C, G, K) or in the presence of both inhibitors (D, H, L). [^{3}H]Sunitinib was applied at initial concentrations of 0.2 μM (A−D), 2.0 μM (E−H) and 20 μM (I−L) to either apical or basolateral compartments. Note that no significant polarized sunitinib transport was observed in parental MDCKII cells, indicating a negligible transport contribution of endogenous canine ABCB1 (data not shown). Translocation from the apical to the basolateral compartment (open circles), translocation from the basolateral to the apical compartment (filled squares). Results are expressed as mean values ($n = 3$) of relative transport (%) ± SD (error bars are frequently within the symbols). The transport ratio (r) was calculated as described with Figure 2. Differences at 4 h were tested by Student's t test (**: $p < 0.01$, ***: $p < 0.001$).

Ko143 or zosuquidar, respectively, indicating a dominant role of ABCG2 in the efflux of sorafenib out of the cells at 0.3 μM. Coincubation with Ko143 and zosuquidar caused a 7.2-fold increase in cellular sorafenib accumulation. Saturation of ABCB1-mediated

dx.doi.org/10.1021/mp1003898 |*Mol. Pharmaceutics* 2011, 8, 571–582

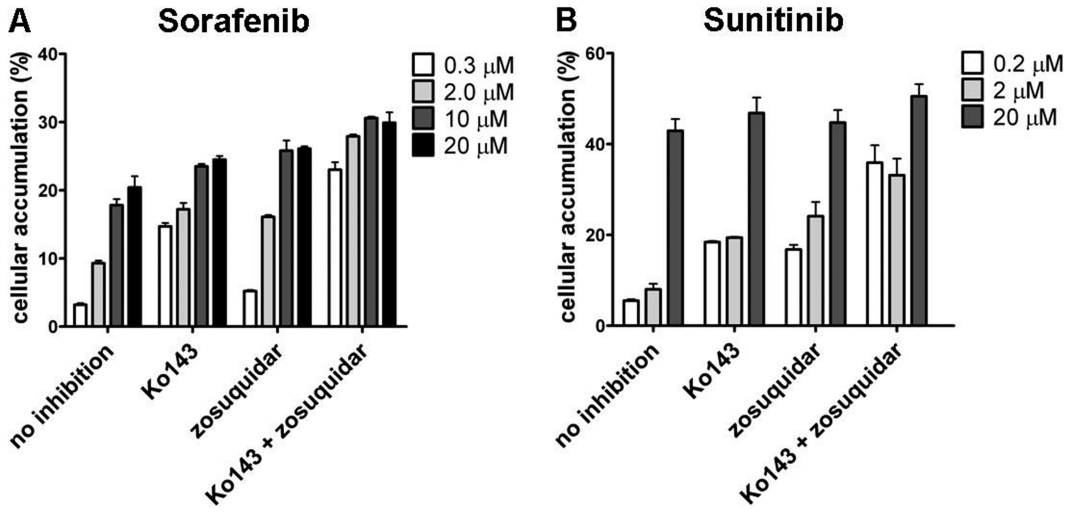

Figure 6. Cellular accumulation of [^{3}H]sorafenib (A) and [^{3}H]sunitinib (B) in MDCKII-ABCB1/ABCG2 cells. The drugs were applied in the apical compartment at initial concentrations of 0.3, 2, 10, and 20 μM for sorafenib, and at 0.2, 2, and 20 μM for sunitinib. After 4 h cells were washed and the radioactivity in the filters was determined. Results are expressed as mean values (n = 3) of relative radioactivity (%) compared to the initially applied amount of drug ± SD.

efflux as judged from cellular accumulation (Ko143 data) became evident at a sorafenib concentration of 10 μM, while for ABCG2 (zosuquidar data) beginning saturation was already found at 2.0 μM. These results are in line with the transcellular transport data indicating that ABCG2 is the major determinant for cellular efflux transport of sorafenib at low concentrations, whereas ABCB1 is more important at high concentrations.

For sunitinib we found intracellular accumulation of 5.5% at 0.2 μM, in the absence of inhibitors (Figure 6B). Addition of either Ko143 or zosuquidar resulted in 3.3- and 3.0-fold higher cellular accumulation, respectively, pointing to an equal contribution of ABCB1 and ABCG2 to sunitinib efflux. Coincubation with both inhibitors resulted in 6.5-fold increased intracellular sunitinib concentrations. At a sunitinib concentration of 2 μM the relative cellular accumulation was modestly increased compared to 0.2 μM in the absence of inhibitors or in the presence of zosuquidar, but not with Ko143, suggesting beginning saturation of ABCG2 but not of ABCB1. At a further increased sunitinib concentration of 20 μM cellular accumulation was found to be in between 43 and 50% in the absence or in the presence of one or both inhibitors. Although this finding suggests near saturation of both transporters at 20 μM, we still observed transport ratios between 1.3 and 2.2 unless both inhibitors were applied (Figure 5I−L), presumably resulting mainly from remaining ABCB1-mediated transport acivity. Taken together, the cellular accumulation results for sorafenib and sunitinib largely reflect the transcellular transport data.

DISCUSSION

In this study we describe the generation and characterization of a double-transduced MDCKII cell line overexpressing human ABCB1 and ABCG2. Transduction of the MDCKII-ABCB1 cell line with human ABCG2 resulted in a clone with stable expression of significant ABCG2 and ABCB1 protein levels and efficient transport activity for several test drugs. In parallel we generated a new MDCKII cell line with stable overexpression of ABCG2. Next, we used the ABCB1/ABCG2 cell line to study the interplay between ABCB1 and ABCG2 in terms of transepithelial translocation of the shared substrates topotecan, sorafenib and sunitinib. The use of specific inhibitors of ABCB1 and ABCG2 allowed us to study the single and the combined contribution of both efflux transporters to the translocation of the tested substrates. Furthermore, as discussed below, the chosen approach enabled us to compare our *in vitro* results with previously generated brain penetration data for topotecan, sorafenib and sunitinib in WT, *Abcb1a/1b*$^{-/-}$ and *Abcg2*$^{-/-}$ single and *Abcb1a/1b;Abcg2*$^{-/-}$ combination knockout mice.[7,11] The results indicate a good qualitative correlation between the *in vitro* and *in vivo* data, suggesting that the developed model will help us to better understand the ABCB1/ABCG2 interplay in the BBB.

The topoisomerase I inhibitor topotecan is a well-known cosubstrate of murine and human ABCB1 and ABCG2.[23−25] Using single transporter-overexpressing MDCKII cells, Li et al. reported partially saturable topotecan transport by ABCB1 and ABCG2[26] and Muenster and coauthors found partial saturation of the murine Abcg2 for topotecan concentrations up to 500 μM.[27] This is in agreement with our observation in the ABCB1/ABCG2 cell line, where the activity of both transport proteins was partially reduced to the same extent at 500 μM topotecan, most likely due to beginning saturation of the efflux transporters. Recently, de Vries et al. analyzed the combined role of ABCB1 and ABCG2 in limiting the brain penetration of topotecan in WT, *Abcb1a/1b*$^{-/-}$, *Abcg2*$^{-/-}$ and *Abcb1a/1b;Abcg2*$^{-/-}$ mice.[7] In the mouse strain lacking both transporters, the topotecan AUC_{brain} over a period of 24 h was 12-fold increased compared to WT mice, whereas in *Abcg2*$^{-/-}$ and *Abcb1a/1b*$^{-/-}$ mice, the AUC_{brain} was only 1.5-fold and 1.6-fold higher, respectively (Figure 7C). Qualitatively similar-fold differences among the mouse strains were also measured at 1 and 4 h.

For a more straightforward comparison with *in vivo* brain penetration data we converted the *in vitro* transport ratios (basolateral-to-apical transport divided by apical-to-basolateral transport, BA/AB, or r) to inverse transport ratios (AB/BA, or 1/r) (Figure 7). Since high apically directed drug transport by ABCB1 and ABCG2 counteracts brain penetration of drugs, inverse transport ratios correlate more directly with the *in vivo* drug uptake across the BBB. Indeed, also the *in vitro* cellular drug accumulation profiles

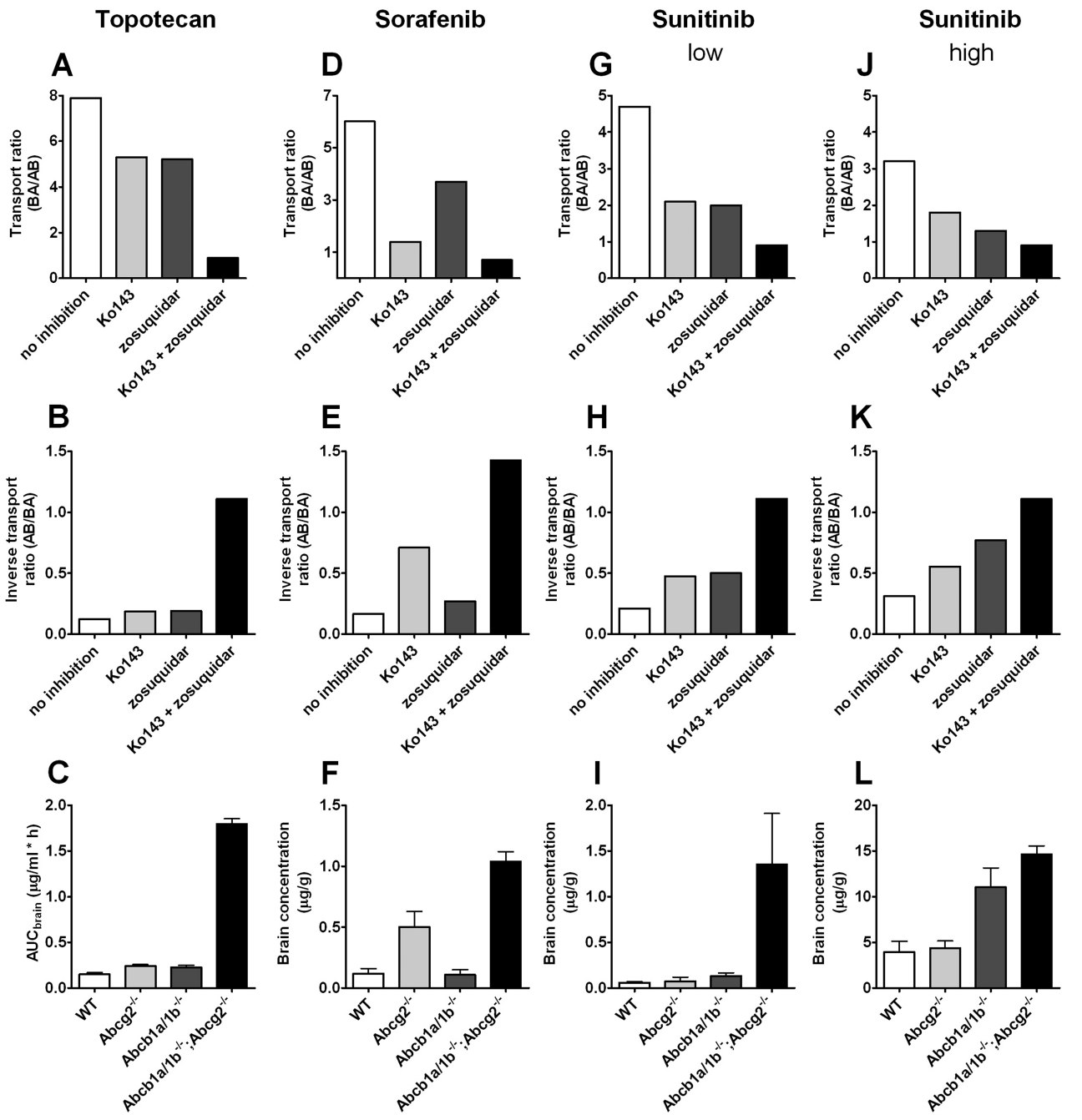

Figure 7. Comparison of *in vitro* transport ratios and inverse transport ratios of topotecan (A, B), sorafenib (D, E) and sunitinib (G, H, J, K) in MDCKII-ABCB1/ABCG2 cell with *in vivo* brain concentrations of topotecan (C), sorafenib (F) and sunitinib (I, L) in WT, *Abcg2*$^{-/-}$, *Abcb1a/1b*$^{-/-}$ and *Abcb1a/1b;Abcg2*$^{-/-}$ mice. *In vitro*, topotecan was applied at 1.6 μM, sorafenib at 0.3 μM (D, E) and sunitinib at 0.2 μM (G, H) or 2.0 μM (J, K). Basolaterally directed translocation data (AB) and apically directed translocation data (BA) of the drugs were used to calculate transport ratios (BA/AB) and inverse transport ratios (AB/BA). Experiments were performed either in absence of any inhibitor (white bars), in the presence of 1 μM Ko143 (light gray bars), 5 μM zosuquidar (dark gray bars) or in the presence of both in inhibitors simultaneously (black bars). Results are expressed as mean values (n = 3). Brain penetration data were taken from the literature (de Vries et al., 2007;[7] Lagas et al., 2010;[11] Tang et al., 2011[15]). Topotecan data are presented as AUC_{brain} (ng/mL * h over a 24 h period; mean of n = 25 per cohort ± SE) after intravenous administration of 5 mg/kg (C). Sorafenib brain concentrations (μg/g; n = 5 ± SD) were measured 6 h after oral administration at 10 mg/kg (F). Sunitinib brain concentrations (μg/g; n = 5−8 ± SD) were measured 6 h after oral administration at 10 mg/kg (I) or 10 min after intravenous injection of 20 mg/kg (L).

established at 0.2−2 μM for sorafenib and sunitinib in the various MDCKII lines are a near-perfect mirror of the inverse transport ratio profiles (Supplemental Figure 1 in the Supporting Information). For topotecan the inverse transport ratios at a concentration of 1.6 μM revealed a qualitatively very similar pattern as found for *in vivo* brain AUCs, with a disproportionate 8.8-fold increase when both transporters were blocked, while inhibition of only one of each transporter led to a 1.5-fold increase (Figure 7B,C). At 500 μM topotecan a qualitatively similar pattern was observed, but the relative differences among the various conditions were reduced due to beginning

dx.doi.org/10.1021/mp1003898 |*Mol. Pharmaceutics* 2011, 8, 571–582

saturation of active transport (Figure 3E−H). Taken together, these findings suggest that, for topotecan, ABCB1 as well as ABCG2 has the ability to compensate for the loss of the other transporter to a similar degree both *in vitro* and *in vivo*. The correlation of the 1.6 μM *in vitro* data with the brain penetration data also suggests that the BBB transporters were not significantly saturated *in vivo*.

For the second-generation TKI sorafenib the *in vitro* transport data in ABCB1/ABCG2 cells match the results of Lagas et al. (2010), who found sorafenib to be a weak ABCB1, but a moderate human ABCG2 and a good mouse Abcg2 substrate. Also Hu et al. reported saturable sorafenib transport by human ABCB1 *in vitro*, but they found no significant transport of sorafenib in Saos-2 cells overexpressing ABCG2,[22] perhaps due to relatively low expression of ABCG2 in the cell line used. We further found that sorafenib was transported with different affinities by ABCB1 and ABCG2. At low concentrations, ABCG2 had a significantly higher impact on sorafenib translocation than ABCB1. However, ABCG2 was completely saturated at a concentration of 10 μM, while ABCB1 was still fully active. Hence, there is a shift toward ABCB1-mediated transport at higher sorafenib concentrations.

Lagas et al. (2010) reported no change in relative brain concentrations of sorafenib in Abcb1-deficient mice, but 4.2- and 8.7-fold increases in *Abcg2*$^{-/-}$ and *Abcb1a/1b;Abcg2*$^{-/-}$ mice, respectively, compared with WT mice (Figure 7F), suggesting a major role of Abcg2 in limiting sorafenib brain penetration.[11] Correction of brain concentrations for plasma concentrations did not affect the results, as sorafenib plasma concentrations were comparable in all mouse strains. Like for topotecan, we found a highly similar profile for the inverse transport ratios in ABCB1/ABCG2 cells at low sorafenib concentrations (0.3 μM), showing a major contribution of ABCG2 in limiting sorafenib translocation, especially when ABCB1 was inactive (Figure 7D,E). Sorafenib translocation was 4.2- and 1.6-fold increased when ABCG2 or ABCB1 were blocked, respectively, whereas inhibition of both transporters resulted in an 8.6-fold increased translocation. At a sorafenib concentration of 2 μM the relative pattern among the distinct groups was similar but relative differences were lower (Figure 4E−H).

The *in vitro* data obtained by us and by Lagas et al. indicate that sorafenib is only a moderate substrate for ABCB1 *in vitro*.[11] This finding can explain the increased brain accumulation in single *Abcg2*$^{-/-}$ mice, whereas Abcg2 can completely compensate for the loss of Abcb1. As our results demonstrate saturation of ABCG2 at higher sorafenib concentrations it can be speculated that sorafenib relative brain accumulation in *Abcb1a/1b*$^{-/-}$ mice might increase when sorafenib is applied at higher doses. However, the plasma concentrations needed may be difficult to achieve in clinically realistic situations (see below).

We recently demonstrated that the TKI sunitinib is a shared substrate of ABCB1 and ABCG2 *in vitro* and *in vivo*, and an efficiently transported substrate of murine Abcg2.[15] Here we show that sunitinib is a moderate *in vitro* substrate of human ABCB1 and ABCG2. Tang et al. further observed a 23.4-fold increased sunitinib brain concentration in *Abcb1a/1b;Abcg2*$^{-/-}$ mice compared to WT mice 6 h after oral administration at a dose of 10 mg/kg, while the brain accumulation was only marginally increased in *Abcg2*$^{-/-}$ and *Abcb1a/1b*$^{-/-}$ mice, by 1.3- and 2.3-fold, respectively (Figure 7I). This indicates that Abcg2 and Abcb1 can largely compensate for each other's absence at this exposure level. However, when, in an effort to saturate the BBB transporters, sunitinib was administered intravenously at a maximum tolerable dose of 20 mg/kg and brain concentrations were measured 10 min after administration, only 3.7-fold and 2.8-fold increases were found in *Abcb1a/1b;Abcg2*$^{-/-}$ and *Abcb1a/1b*$^{-/-}$ mice, respectively, compared to WT mice (Figure 7L).[15] In contrast, Abcg2$^{-/-}$ mice did not have significantly different sunitinib brain levels from WT mice. These data suggest saturation of Abcg2 in the absence of Abcb1 at high sunitinib levels, whereas Abcb1 could still fully compensate for the loss of Abcg2.

The inverse transport ratios obtained in MDCKII-ABCB1/ABCG2 cells again revealed a qualitatively similar pattern for sunitinib *in vitro* at 0.2 μM and 2 μM and *in vivo* brain penetration under low and high exposure conditions, with saturation of Abcg2 becoming obvious at high exposure levels both *in vitro* and *in vivo* (Figure 7H,I,K,L). However, the impact of losing ABCG2 activity alone was more apparent *in vitro* (Ko143 inhibition results) than in the *in vivo* brain penetration results. Possibly for sunitinib human ABCG2 has a relatively higher impact compared to human ABCB1 than mouse Abcg2 vs mouse Abcb1. The lower fold-difference between uninhibited and coinhibited conditions in MDCKII-ABCB1/ABCG2 cells at 0.2 μM than between WT and *Abcb1a/1b;Abcg2*$^{-/-}$ brains at low exposure (Figure 7H, I) might result from a higher overall background permeability for sunitinib in MDCKII cells compared to the BBB in mice under low exposure conditions. This would reduce the overall impact of efflux transporters on transport ratios.

After initiation of the present study, Kodaira et al. published a kinetic analysis of previously reported brain accumulation data of several drugs including TKIs.[14] The disproportionate brain accumulation of shared ABCB1 and ABCG2 substrates observed in *Abcb1a/1b;Abcg2*$^{-/-}$ mice compared to *Abcb1a/1b*$^{-/-}$ and *Abcg2*$^{-/-}$ mice could be explained in a straightforward manner by the additive contribution of Abcb1 and Abcg2 to the net efflux at the BBB, and by the fact that the intrinsic efflux activities of ABCB1 and ABCG2 were each much larger than the remaining (most likely passive) efflux activity at the BBB. The authors concluded that there is no need to postulate a direct synergistic interaction between ABCB1 and ABCG2. Although outside of our expertise, it is likely that this kinetic model can also be applied to the results obtained with the MDCKII-ABCB1/ABCG2 cells.

Our results for topotecan, sorafenib and sunitinib obtained in the MDCKII-ABCB1/ABCG2 cell line depict a highly similar qualitative pattern when compared with the corresponding brain accumulation data derived from mouse experiments. This suggests that the MDCKII-ABCB1/ABCG2 cell line is a useful *in vitro* model to qualitatively mimic the effects of both transporters on brain penetration across the BBB. However, making a direct quantitative prediction for the brain accumulation in mice or in humans based on our *in vitro* results will remain more complicated. Possible limitations are mouse-human species differences in substrate affinities, and the unknown absolute protein expression of ABCB1 and ABCG2 in the MDCKII cell line compared to that in murine and human BBB. Only recently Kamiie and coauthors developed a method for absolute quantification of membrane transporter proteins in mice by liquid chromatography-tandem mass spectrometry.[28] Applying this approach to MDCKII-ABCB1/ABCG2 cells and freshly isolated human BCECs may allow a more quantitative comparison of transporter expression. Furthermore, the MDCKII cell line, which is derived from kidney tubular epithelium, may exhibit different characteristics from BCECs, affecting the background permeability for test

compounds. Nevertheless, in a study by Garberg et al.[29] comparing several BBB *in vitro* models, including isolated primary BCECs, several BBB cell lines, Caco-2 and MDCKII parental and -ABCB1 cells for their usefulness in discriminating between compounds with passive diffusion and active efflux, best results were obtained for primary BCECs and MDCKII-ABCB1 cells. Furthermore, inulin permeability was found to be lowest in Caco-2 and MDCKII cells followed by primary bovine BCECs. Still, in comparison with mouse brain uptake data, the inulin permeability in MDCKII cells was ~10 times higher. This study demonstrated that high transporter expression and activity as well as low paracellular permeability are crucial factors for a useful BBB *in vitro* model.[29] In the past, many BBB cell lines, mainly of animal origin, failed to form tight monolayers, or expressed drug transporters only at low levels.[30−32] Recently, human BBB cell lines were developed which exhibit paracellular resistance close to that of primary BCECs.[33,34] However, despite the detected expression of the relevant efflux transporters, transport activity was only found for very good ABCB1 or ABCG2 substrates. For this reason, isolated primary BCECs of different origin are often still the preferred *in vitro* models to study efflux transport. However, Garberg et al. concluded that a specific *in vitro* model of the BBB is not needed when the main focus is the study of permeability and brain distribution of ABCB1 substrate drugs. It should be noted, though, that no substrates with high affinities to ABCG2 were included in that study. Thus, by integrating ABCG2 into the MDCKII-ABCB1 cell line, we have increased its application range for substrates of the human ABCG2, while its barrier properties and ABCB1 activity remain preserved.

■ ASSOCIATED CONTENT

Supporting Information. Supplemental Figure 1 depicting comparison of inverse transport ratios with cellular accumulation of sorafenib and sunitinib in MDCKII-ABCB1/ABCG2 cells. This material is available free of charge via the Internet at http://pubs.acs.org.

■ AUTHOR INFORMATION

Corresponding Author

*The Netherlands Cancer Institute, Division of Molecular Biology, Plesmanlaan 121, 1066 CX Amsterdam, The Netherlands. E-mail: a.schinkel@nki.nl. Phone: +31 20 5122046. Fax: +31 20 669 1383.

■ ACKNOWLEDGMENT

We gratefully acknowledge the help and advice of Dr. Conchita Vens for the transduction process. We also acknowledge a postdoctoral fellowship from the Swiss National Science Foundation to B.P. [PBBSP3-128567] and an academic staff training scheme fellowship from the Malaysian Ministry of Science, Technology and Innovation to S.C.T.

■ ABBREVIATIONS USED

BBB, blood−brain barrier; BCECs, brain capillary endothelial cells; TKI, tyrosine kinase inhibitor; ABC transporter, ATP-binding cassette transporter

■ REFERENCES

(1) Schinkel, A. H.; Jonker, J. W. Mammalian drug efflux transporters of the ATP binding cassette (ABC) family: an overview. *Adv. Drug Delivery Rev.* **2003**, *55* (1), 3–29.

(2) Borst, P.; Oude Elferink, R. P. Mammalian ABC transporters in health and disease. *Annu. Rev. Biochem.* **2002**, *71*, 537–92.

(3) Schinkel, A. H.; Smit, J. J.; van Tellingen, O.; Beijnen, J. H.; Wagenaar, E.; van Deemter, L.; Mol, C. A.; van der Valk, M. A.; Robanus-Maandag, E. C.; te Riele, H. P.; et al. Disruption of the mouse mdr1a P-glycoprotein gene leads to a deficiency in the blood-brain barrier and to increased sensitivity to drugs. *Cell* **1994**, *77* (4), 491–502.

(4) Kemper, E. M.; van Zandbergen, A. E.; Cleypool, C.; Mos, H. A.; Boogerd, W.; Beijnen, J. H.; van Tellingen, O. Increased penetration of paclitaxel into the brain by inhibition of P-Glycoprotein. *Clin. Cancer Res.* **2003**, *9* (7), 2849–55.

(5) Breedveld, P.; Pluim, D.; Cipriani, G.; Wielinga, P.; van Tellingen, O.; Schinkel, A. H.; Schellens, J. H. The effect of Bcrp1 (Abcg2) on the in vivo pharmacokinetics and brain penetration of imatinib mesylate (Gleevec): implications for the use of breast cancer resistance protein and P-glycoprotein inhibitors to enable the brain penetration of imatinib in patients. *Cancer Res.* **2005**, *65* (7), 2577–82.

(6) Cisternino, S.; Mercier, C.; Bourasset, F.; Roux, F.; Scherrmann, J. M. Expression, up-regulation, and transport activity of the multidrug-resistance protein Abcg2 at the mouse blood-brain barrier. *Cancer Res.* **2004**, *64* (9), 3296–301.

(7) de Vries, N. A.; Zhao, J.; Kroon, E.; Buckle, T.; Beijnen, J. H.; van Tellingen, O. P-glycoprotein and breast cancer resistance protein: two dominant transporters working together in limiting the brain penetration of topotecan. *Clin. Cancer Res.* **2007**, *13* (21), 6440–9.

(8) Oostendorp, R. L.; Buckle, T.; Beijnen, J. H.; van Tellingen, O.; Schellens, J. H. The effect of P-gp (Mdr1a/1b), BCRP (Bcrp1) and P-gp/BCRP inhibitors on the in vivo absorption, distribution, metabolism and excretion of imatinib. *Invest. New Drugs* **2009**, *27* (1), 31–40.

(9) Polli, J. W.; Humphreys, J. E.; Harmon, K. A.; Castellino, S.; O'Mara, M. J.; Olson, K. L.; John-Williams, L. S.; Koch, K. M.; Serabjit-Singh, C. J. The role of efflux and uptake transporters in [N-{3-chloro-4-[(3-fluorobenzyl)oxy]phenyl}-6-[5-({[2-(methylsulfonyl)ethyl]amino}-methyl)-2-furyl]-4-quinazolinamine (GW572016, lapatinib) disposition and drug interactions. *Drug Metab. Dispos.* **2008**, *36* (4), 695–701.

(10) Lagas, J. S.; van Waterschoot, R. A.; van Tilburg, V. A.; Hillebrand, M. J.; Lankheet, N.; Rosing, H.; Beijnen, J. H.; Schinkel, A. H. Brain accumulation of dasatinib is restricted by P-glycoprotein (ABCB1) and breast cancer resistance protein (ABCG2) and can be enhanced by elacridar treatment. *Clin. Cancer Res.* **2009**, *15* (7), 2344–51.

(11) Lagas, J. S.; van Waterschoot, R. A.; Sparidans, R. W.; Wagenaar, E.; Beijnen, J. H.; Schinkel, A. H. Breast cancer resistance protein and P-glycoprotein limit sorafenib brain accumulation. *Mol. Cancer Ther.* **2010**, *9* (2), 319–26.

(12) Agarwal, S.; Sane, R.; Gallardo, J. L.; Ohlfest, J. R.; Elmquist, W. F. Distribution of gefitinib to the brain is limited by P-glycoprotein (ABCB1) and breast cancer resistance protein (ABCG2)-mediated active efflux. *J. Pharmacol. Exp. Ther.* **2010**, *334* (1), 147–55.

(13) Marchetti, S.; de Vries, N. A.; Buckle, T.; Bolijn, M. J.; van Eijndhoven, M. A.; Beijnen, J. H.; Mazzanti, R.; van Tellingen, O.; Schellens, J. H. Effect of the ATP-binding cassette drug transporters ABCB1, ABCG2, and ABCC2 on erlotinib hydrochloride (Tarceva) disposition in in vitro and in vivo pharmacokinetic studies employing Bcrp1−/−/Mdr1a/1b−/− (triple-knockout) and wild-type mice. *Mol. Cancer Ther.* **2008**, *7* (8), 2280–7.

(14) Kodaira, H.; Kusuhara, H.; Ushiki, J.; Fuse, E.; Sugiyama, Y. Kinetic analysis of the cooperation of P-glycoprotein (P-gp/Abcb1) and breast cancer resistance protein (Bcrp/Abcg2) in limiting the brain and testis penetration of erlotinib, flavopiridol, and mitoxantrone. *J. Pharmacol. Exp. Ther.* **2010**, *333* (3), 788–96.

(15) Tang, S. C.; Lagas, J. S.; Lankheet, N.; Poller, B.; Rosing, H.; Beijnen, J. H.; Schinkel, A. H. Brain accumulation of sunitinib is restricted by P-glycoprotein (ABCB1) and Breast Cancer Resistance Protein (ABCG2) and can be enhanced by oral elacridar and sunitinib coadministration. *Int. J. Cancer* **2011**, in press.

(16) Allen, J. D.; van Loevezijn, A.; Lakhai, J. M.; van der Valk, M.; van Tellingen, O.; Reid, G.; Schellens, J. H.; Koomen, G. J.; Schinkel, A. H. Potent and specific inhibition of the breast cancer resistance

protein multidrug transporter in vitro and in mouse intestine by a novel analogue of fumitremorgin C. *Mol. Cancer Ther.* **2002**, *1* (6), 417–25.

(17) Pavek, P.; Merino, G.; Wagenaar, E.; Bolscher, E.; Novotna, M.; Jonker, J. W.; Schinkel, A. H. Human breast cancer resistance protein: interactions with steroid drugs, hormones, the dietary carcinogen 2-amino-1-methyl-6-phenylimidazo(4,5-b)pyridine, and transport of cimetidine. *J. Pharmacol. Exp. Ther.* **2005**, *312* (1), 144–52.

(18) Evers, R.; Cnubben, N. H.; Wijnholds, J.; van Deemter, L.; van Bladeren, P. J.; Borst, P. Transport of glutathione prostaglandin A conjugates by the multidrug resistance protein 1. *FEBS Lett.* **1997**, *419* (1), 112–6.

(19) Merino, G.; Alvarez, A. I.; Pulido, M. M.; Molina, A. J.; Schinkel, A. H.; Prieto, J. G. Breast cancer resistance protein (BCRP/ABCG2) transports fluoroquinolone antibiotics and affects their oral availability, pharmacokinetics, and milk secretion. *Drug Metab. Dispos.* **2006**, *34* (4), 690–5.

(20) van Herwaarden, A. E.; Wagenaar, E.; Karnekamp, B.; Merino, G.; Jonker, J. W.; Schinkel, A. H. Breast cancer resistance protein (Bcrp1/Abcg2) reduces systemic exposure of the dietary carcinogens aflatoxin B1, IQ and Trp-P-1 but also mediates their secretion into breast milk. *Carcinogenesis* **2006**, *27* (1), 123–30.

(21) Bakos, E.; Evers, R.; Szakacs, G.; Tusnady, G. E.; Welker, E.; Szabo, K.; de Haas, M.; van Deemter, L.; Borst, P.; Varadi, A.; Sarkadi, B. Functional multidrug resistance protein (MRP1) lacking the N-terminal transmembrane domain. *J. Biol. Chem.* **1998**, *273* (48), 32167–75.

(22) Hu, S.; Chen, Z.; Franke, R.; Orwick, S.; Zhao, M.; Rudek, M. A.; Sparreboom, A.; Baker, S. D. Interaction of the multikinase inhibitors sorafenib and sunitinib with solute carriers and ATP-binding cassette transporters. *Clin. Cancer Res.* **2009**, *15* (19), 6062–9.

(23) Jonker, J. W.; Smit, J. W.; Brinkhuis, R. F.; Maliepaard, M.; Beijnen, J. H.; Schellens, J. H.; Schinkel, A. H. Role of breast cancer resistance protein in the bioavailability and fetal penetration of topotecan. *J. Natl. Cancer Inst.* **2000**, *92* (20), 1651–6.

(24) Kruijtzer, C. M.; Beijnen, J. H.; Rosing, H.; ten Bokkel Huinink, W. W.; Schot, M.; Jewell, R. C.; Paul, E. M.; Schellens, J. H. Increased oral bioavailability of topotecan in combination with the breast cancer resistance protein and P-glycoprotein inhibitor GF120918. *J. Clin. Oncol.* **2002**, *20* (13), 2943–50.

(25) Maliepaard, M.; van Gastelen, M. A.; de Jong, L. A.; Pluim, D.; van Waardenburg, R. C.; Ruevekamp-Helmers, M. C.; Floot, B. G.; Schellens, J. H. Overexpression of the BCRP/MXR/ABCP gene in a topotecan-selected ovarian tumor cell line. *Cancer Res.* **1999**, *59* (18), 4559–63.

(26) Li, H.; Jin, H. E.; Kim, W.; Han, Y. H.; Kim, D. D.; Chung, S. J.; Shim, C. K. Involvement of P-glycoprotein, multidrug resistance protein 2 and breast cancer resistance protein in the transport of belotecan and topotecan in Caco-2 and MDCKII cells. *Pharm. Res.* **2008**, *25* (11), 2601–12.

(27) Muenster, U.; Grieshop, B.; Ickenroth, K.; Gnoth, M. J. Characterization of substrates and inhibitors for the in vitro assessment of Bcrp mediated drug-drug interactions. *Pharm. Res.* **2008**, *25* (10), 2320–6.

(28) Kamiie, J.; Ohtsuki, S.; Iwase, R.; Ohmine, K.; Katsukura, Y.; Yanai, K.; Sekine, Y.; Uchida, Y.; Ito, S.; Terasaki, T. Quantitative atlas of membrane transporter proteins: development and application of a highly sensitive simultaneous LC/MS/MS method combined with novel in-silico peptide selection criteria. *Pharm. Res.* **2008**, *25* (6), 1469–83.

(29) Garberg, P.; Ball, M.; Borg, N.; Cecchelli, R.; Fenart, L.; Hurst, R. D.; Lindmark, T.; Mabondzo, A.; Nilsson, J. E.; Raub, T. J.; Stanimirovic, D.; Terasaki, T.; Oberg, J. O.; Osterberg, T. In vitro models for the blood-brain barrier. *Toxicol. in Vitro* **2005**, *19* (3), 299–334.

(30) Kusch-Poddar, M.; Drewe, J.; Fux, I.; Gutmann, H. Evaluation of the immortalized human brain capillary endothelial cell line BB19 as a human cell culture model for the blood-brain barrier. *Brain Res.* **2005**, *1064* (1−2), 21–31.

(31) Omidi, Y.; Campbell, L.; Barar, J.; Connell, D.; Akhtar, S.; Gumbleton, M. Evaluation of the immortalised mouse brain capillary endothelial cell line, b.End3, as an in vitro blood-brain barrier model for drug uptake and transport studies. *Brain Res.* **2003**, *990* (1−2), 95–112.

(32) Roux, F.; Couraud, P. O. Rat brain endothelial cell lines for the study of blood-brain barrier permeability and transport functions. *Cell. Mol. Neurobiol.* **2005**, *25* (1), 41–58.

(33) Sano, Y.; Shimizu, F.; Abe, M.; Maeda, T.; Kashiwamura, Y.; Ohtsuki, S.; Terasaki, T.; Obinata, M.; Kajiwara, K.; Fujii, M.; Suzuki, M.; Kanda, T. Establishment of a new conditionally immortalized human brain microvascular endothelial cell line retaining an in vivo blood-brain barrier function. *J. Cell. Physiol.* **2010**, *225* (2), 519–28.

(34) Weksler, B. B.; Subileau, E. A.; Perriere, N.; Charneau, P.; Holloway, K.; Leveque, M.; Tricoire-Leignel, H.; Nicotra, A.; Bourdoulous, S.; Turowski, P.; Male, D. K.; Roux, F.; Greenwood, J.; Romero, I. A.; Couraud, P. O. Blood-brain barrier-specific properties of a human adult brain endothelial cell line. *FASEB J.* **2005**, *19* (13), 1872–4.